J. Chem. Sci. Vol. 126, No. 6, November 2014, pp. 1789–1801.

A computational study on kinetics, mechanism and thermochemistry of gas-phase reactions of 3-hydroxy-2-butanone with OH radicals

NAND KISHOR GOUR[a], SATYENDRA GUPTA[a], BHUPESH KUMAR MISHRA[b,*] and HARI JI SINGH[a,*]

[a]Department of Chemistry, D. D.U. Gorakhpur University Gorakhpur, Uttar Pradesh, 273 009, India
[b]Department of Chemical Sciences, Tezpur University Tezpur, Assam, 784 028, India
e-mail: bhupesh@tezu.ernet.in; hjschem50@gmail.com

MS received 13 March 2014; revised 26 May 2014; accepted 09 June 2014

Abstract. Theoretical investigation has been carried out on the kinetics and reaction mechanism of the gas-phase reaction of 3-hydroxy-2-butanone (3H2B) with OH radical using dual-level procedure employing the optimization at DFT(BHandHLYP)/6-311++G(d,p) followed by a single-point energy calculation at the CCSD(T)/6-311++G(d,p) level of theory. The pre- and post reactive complexes are also validated at entrance and exit channels, respectively. Thus reaction may be proceed via indirect mechanism. The intrinsic reaction coordinate (IRC) calculation has also been performed to confirm the smooth transition from a reactant to product through the respective transition states. The rate coefficients were calculated for the first time over a wide range of temperature (250–450 K) and described by the following expression: $k_{OH} = 7.56 \times 10^{-11}\exp[-(549.3 \pm 11.2)/T]$ cm^3 molecule^{-1}s^{-1}. At 298 K, our calculated rate coefficient 1.20×10^{-11} cm^3 molecule^{-1} s^{-1} is in good agreement with the experimental results. Our calculation indicates that H-abstraction from α-C-H site of 3H2B is the dominant reaction channel. Using group-balanced isodesmic reactions, the standard enthalpies of formation for 3H2B and radicals generated by hydrogen abstraction are reported for the first time. The branching ratios of the different reaction channels are also determined. Also, the atmospheric lifetime of 3H2B is also calculated to be 1.04 days.

Keywords. Hydroxyketone; bond dissociation energy; isodesmic reactions; atmospheric lifetime.

1. Introduction

Carbonyls are known to be important intermediates in pyrolysis and combustion processes on saturated and unsaturated hydrocarbons.[1,2] Wolfe *et al*.[3] have shown in experimental studies that significant fractions of aldehydes and ketones are formed in the oxidation of isoprene. They are also directly emitted into the troposphere from biogenic[4,5] and anthropogenic sources.[6,7] They play a significant role in atmospheric chemistry due to their strong contribution in the formation of free radicals that are responsible for the oxidation of hydrocarbons.[8] They are precursors of oxidants such as peroxyacyl nitrates (PANs), nitric acid and ozone.[9] Ketones are a major class of organic chemicals and most common pollutants that are widely used in the industry as paints, solvents, etc.[1] They are important in the chemistry of the atmosphere and in combustion systems from direct emissions and as intermediates. α-Hydroxy ketone is a functional group entity of many biologically active natural products such as sugars and antibiotics.[10,11] Furthermore, α-Hydroxy ketones are useful synthones in organic synthesis, with widely studied chemistry.[12,13] The main loss process of hydroxycarbonyl in the troposphere is photolysis and reaction with OH radicals.[14] Several studies[15–20] have been performed on the kinetics and mechanism of the reaction of hydroxyacetone with OH radicals. 3-Hydroxy-2-butanone, also known as acetoin or acetylmethylcarbinol, is a valuable flavour existing naturally in corn, kidney beans, peas and broccoli, and also the common intermediate for diacetyl and 2,3-butanediol synthesis.[21] Wren and Glowa[22] reported that radiolytic decomposition of methyl ethyl ketone produces 3-hydroxy-2-butanone. Aschmann *et al*.[14] studied kinetics of 3H2B with OH radicals at 294 ± 2K and 740 Torr total pressure of purified air using relative rate methods during investigation and reported the rate coefficient, $k_{OH} = 1.03 \times 10^{-11}$ cm^3 molecule^{-1} s^{-1}. Recently, the gas-phase reaction of 3H2B with OH radicals has been studied experimentally by Messaadia *et al*.[23] using the relative rate method and pyrex atmospheric chamber at 600–760 Torr of purified air by employing Smog chamber/FTIR and LP/LIF techniques. The experimental rate

*For correspondence

constant for the reaction 3H2B with OH radicals at 298 K was reported to be (0.96 ± 0.3) × 10^{-11} cm^3 $molecule^{-1}$ s^{-1}.[23] As mentioned above, the study of the gas-phase reaction of 3H2B with atmospheric radicals is presently limited to two investigations at room temperature using the relative rate technique.[14,23] To the best of our knowledge, there is no theoretical study of the title reaction so far. With this stimulus, ab-initio study on the title reaction was performed. 3-hydroxy-2-butanone (3H2B) possesses H atoms under four different environments and therefore the dominant pathways of the abstraction reactions could not be predicted using relative rate method. With this view point, the present study has been undertaken and an attempt has been made to find the dominant pathways and the branching ratio of H-atom abstraction from 3H2B by OH radicals. Our calculations indicate that six reaction channels, four from the two terminals $–CH_3$ groups and two reaction channels each from –CH and –OH groups are feasible as given below:

$CH_3COCH(OH)CH_3 + OH$	→	$CH_2COCH(OH)CH_3 + H_2O$	(R1a and R1b)
	→	$CH_3COC(OH)CH_3 + H_2O$	(*R*2)
	→	$CH_3COCH(O)CH_3 + H_2O$	(*R*3)
	→	$CH_3COCH(OH)CH_2 + H_2O$	(R4a and R4b)

Based on the structure/reactivity relationship using AOPWIN model, it has been reported that –CH attached to hydroxyl group (reaction R2) should be more reactive than the other reaction channels for hydrogen abstraction reactions of 3H2B by OH radical.[23] However, experimental studies provided only the total rate constant and it is difficult to predict the detailed mechanism and thermochemistry. Thus, for a better understanding of mechanistic pathways, kinetics and thermochemistry we must rely on quantum chemical methods. The aim of this paper is to have more accurate thermochemical data on a sound theoretical basis. Our aim is to find out the contribution of the individual channel to the overall rate constant and to provide an understanding of the kinetics involved in the reaction channels (R1–R4). Bond dissociation energies (BDEs) for breaking C-H bonds are known to be strongly correlated with the observed reactivity trend for the hydrogen abstraction reactions. Thus, we present BDE for four types of C-H bonds in 3H2B. In addition, the knowledge of accurate enthalpy of formation ($\Delta_f H^\circ_{298}$) for 3H2B and radicals generated is of vital importance to determine the thermodynamic properties and atmospheric modeling. However, no theoretical or experimental study on standard enthalpy of formation has not been reported so far for these species. Here, we predict the enthalpies of formation using isodesmic reactions by performing single-point energy calculation at high level of theory, CCSD(T) with geometry parameters obtained at the BHandHLYP/6-311++G(d,p) level. Finally, the comparison between theoretical and experimental rate constants is discussed.

2. Computational Methods

Geometry optimization and harmonic vibrational frequency calculation of the species involved in the reaction channels (R1–R4) were performed using hybrid density functional BHandHLYP[24,25] level of theory using Pople's split-valence triple-ζ quality 6-311++G(d,p) basis set with single polarization and double diffuse functions on all atoms. The reactant and product complexes are also validated at the entrance and exit of each reaction channel. The choice of this DFT functional is best exemplified in earlier reports.[26–29] In order to determine the nature of stationary points on the potential energy surface, vibrational frequency calculations were made at the same level of theory. The stationary points were identified to correspond to stable minima on the respective potential energy surface by ascertaining that all the harmonic vibrational frequencies were real and positive. The transition states in reaction channels (R1–R4) were characterized by the presence of only one imaginary frequency (NIMAG=1). At the same level, the minimum energy path (MEP) is obtained by intrinsic reaction coordinates (IRC) calculations.[30] In order to ascertain that the transition of reactants to products via corresponding transition state was smooth, the minimum energy path (MEP) was obtained by intrinsic reaction coordinate (IRC) calculation performed using Gonzales-Schelgel steepest descent path in mass-weighted Cartesian with a gradient step-size of 0.01 ($amu^{1/2}$ –bohr).[30] As the reaction energy barriers are very sensitive to the theoretical levels, the higher-order correlation corrected relative energies along with the density functional

energies are necessary to obtain theoretically consistent reaction energies. Therefore, a potentially high-level method such as couple cluster with single and double excitations including approximate treatment for triple excitations [CCSD(T)][31,32] has been used for single point energy calculations using the same basis set as mentioned above. This dual level method, CCSD(T)// BHandHLYP is known to produce reliable kinetics and energetic results for H-abstraction reactions.[33–36] All the electronic calculations were performed using GAUSSIAN 09 program package.[37]

3. Results and Discussion

The detailed thermodynamic calculation performed at CCSD(T)//BHandHLYP/6-311++G(d,p) level for reaction enthalpies (Δ_rH_{298}) and free energies (Δ_rG_{298}) associated with reaction channels (1–4) are listed in table 1. Free energy values show that four reaction channels are exergonic ($\Delta_rG_{298} < 0$). The Δ_rH_{298} values as recorded in table 1 for reaction channels (R1–R4) reveal that each reaction channels are exothermic in nature and thermodynamic facile. The data given in table 1 suggest that product of reaction R2 is thermodynamically more stable than other reaction channels at 298 K. Thus the hydrogen abstraction for reaction channel R2 may be thermodynamically more favourable than other reaction channels. There are four potential hydrogen abstraction sites of 3H2B, namely the $–CH_3C(O)$, -CH(attached to hydroxyl group), -OH and $–CH_3$ group. It can be seen from the geometrical parameters and stereographical orientation that the hydrogen atoms in the two terminals $–CH_3$ groups are not equivalent. One H-atom is different from the other two in the $– CH_3$ group. Four transition states (TS1a, TS1b, TS4a and TS4b) are therefore located for reaction channels (1 and 4), respectively from the two terminals $–CH_3$ groups. Six transition states (TSs) are therefore, located for reactions of 3H2B with OH radicals. In the entrance channel for reactions R1–R2 pre-reactive complexes (RC1 and RC2) have been validated in the present work. However, for reaction channels R3 and R4, we have found the same reaction complex (RC3/RC4). Similarly, in the exit channels, there are also product complexes occurring before the release of the final products, which are labeled as PC followed by a number (PC1, PC2, PC3 and PC4). In pre-reactive complexes, hydrogen bonds are formed between the oxygen atom of hydroxyl radical with the hydrogen atom in 3H2B with bond distances of 2.726, 2.95, 2.776, 2.02, 3.28 and 2.77 Å, respectively while the other bond lengths are very close to those in equilibrium structures. At the same time, the post-reaction hydrogen bonded complexes (PC1–PC4) with less energy than the corresponding products are located at the exits of the reaction channels (R1–R4) which can be identified with relatively strong C–H...O and O-H...O bonds, as shown in figure 1. So it is clear that the reaction channels (R1–R4) may proceed via indirect mechanisms. The search was made along the minimum energy path on a relaxed potential energy surface. The optimized structures of reactants, reactant complexes, transition states, product complexes and products at BHandHLYP/6-311++G(d,p) level of theory are shown in figure 1. During the formation of transition states, the important structural parameters that have to be observed are one of the C-H bonds of the leaving hydrogen and the newly formed bond between H and O atoms in the OH radical. From figure 1, we can predict that in the optimized structure of transition states (TS1–TS4) for reaction channels (R1–R4), the length of the breaking C-H bonds are found to be longer in the range of 10–15%, whereas the newly formed H-O bond is increased in the range of about 27–36%. The fact that the elongation of forming bond is larger than that of the breaking bond indicates that the barrier of the reactions is near the corresponding reactants. This means the reaction will proceed via early transition state structure which is in consonance with Hammond's postulate[38] applied to an exothermic hydrogen abstraction reaction.

Results obtained during frequency calculations for reactants, products and transition states involved in reaction channels (R1–R4) at BH and HLYP level of theory are recorded in table 2. These results show that the reactants and products have stable minima on their potential energy surface characterized by the occurrence of only real positive vibrational frequencies while transition states TS1a, TS1b, TS2, TS3, TS4a and TS4b are characterized by the occurrence of only one imaginary frequency at 1705i, 2047i, 1086i, 2519i, 2027i and 1654i cm^{-1}, respectively at BHandHLYP level of theory. Visualization of the normal mode associated with the imaginary frequency gives a qualitative

Table 1. Thermochemical data at 298 K for reaction channels (R1–R4) calculated at CCSD(T)/6-311++G(d,p) and BHandHLYP/6-311++G(d,p) (within parentheses) levels of theory. All values are in kcal mol^{-1}.

Reaction channels	$\Delta_rH^\circ_{298}$	$\Delta_rG^\circ_{298}$
Reaction R1	−16.24 (−18.92)	−16.34 (−18.96)
Reaction R2	−28.30 (−32.76)	−29.05 (−33.45)
Reaction R3	−8.64 (−12.23)	−9.06 (−12.59)
Reaction R4	−10.74 (−11.69)	−11.53 (−12.42)

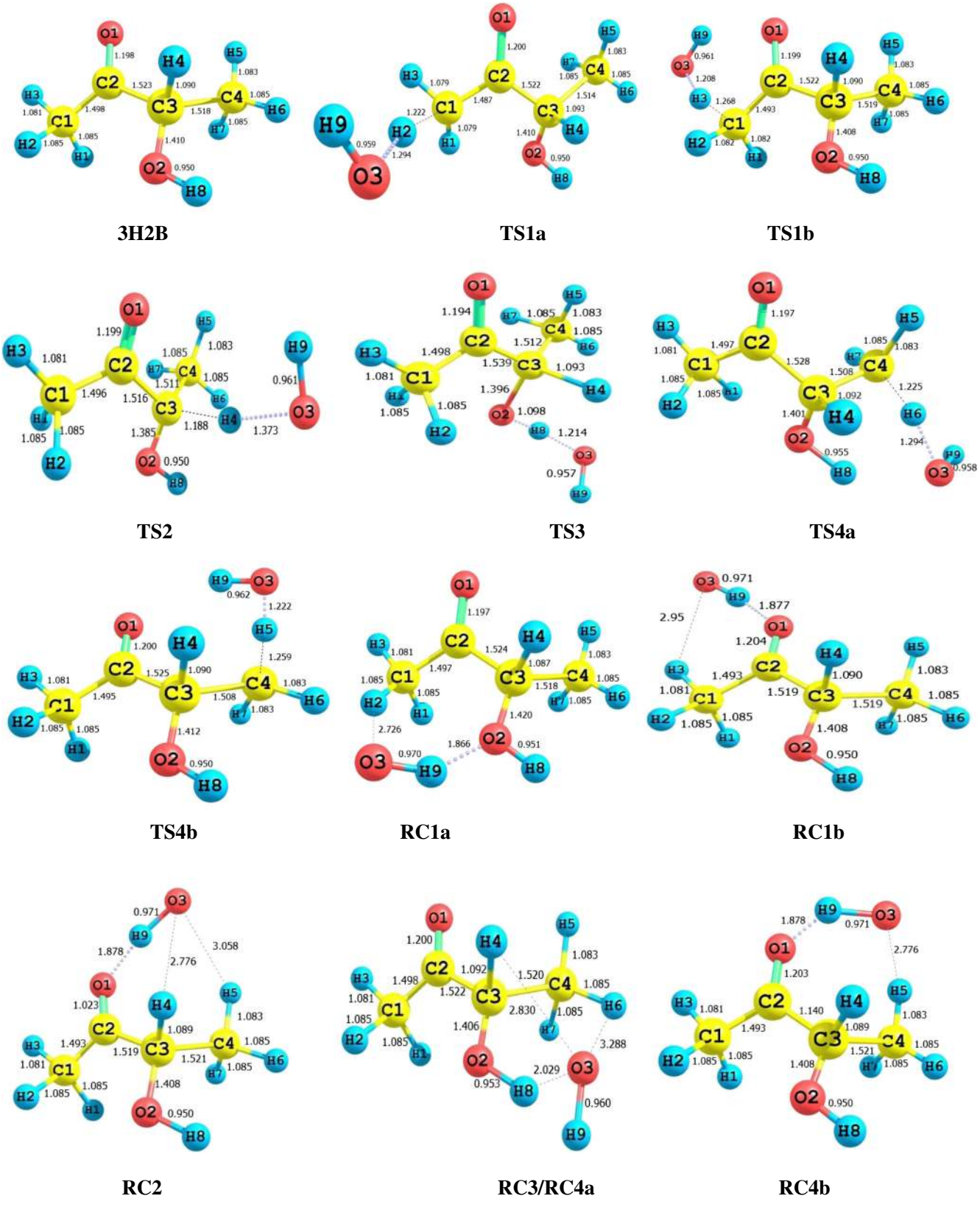

Figure 1. Optimized geometries of reactants, reactant complexes, transition states, product complexes and products involved in the H atom abstraction reactions of 3H2B with OH radicals at BHandHLYP/6-311++G(d,p) level. Bond lengths are given in Å.

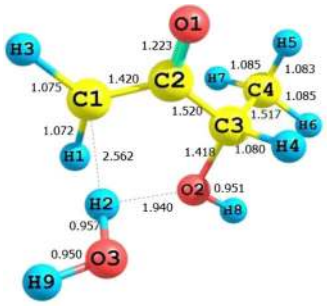

PC1a

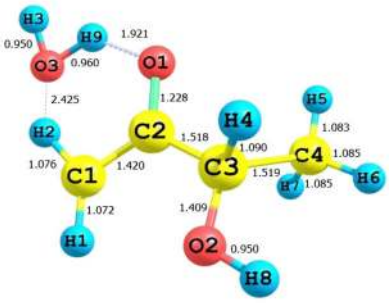

PC1b

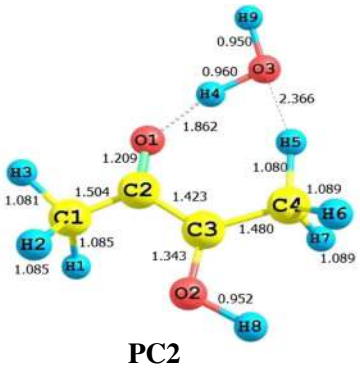

PC2

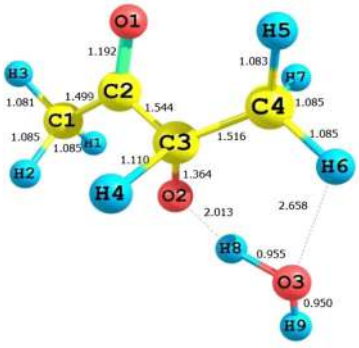

PC3

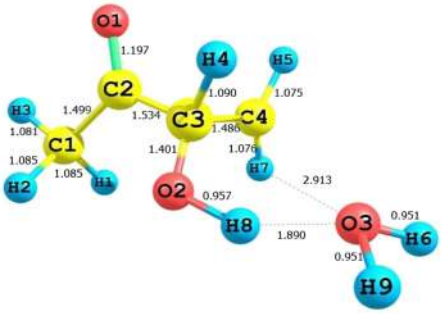

PC4a

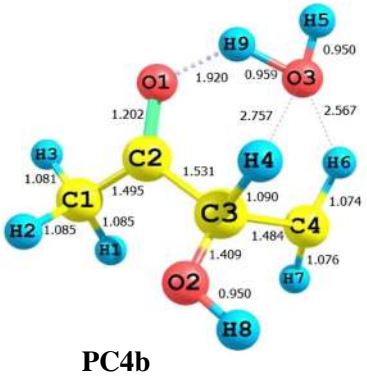

PC4b

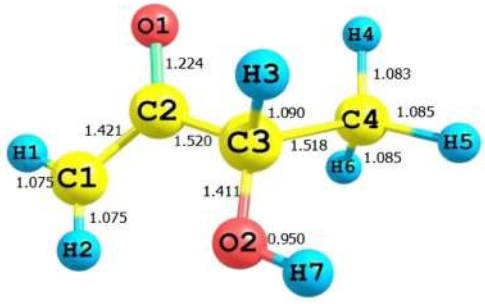

$CH_2COCH(OH)CH_3$ (P1)

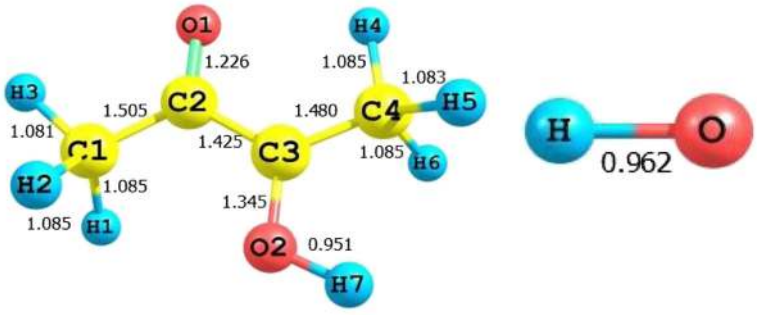

$CH_3COC(OH)CH_3$ (P2)

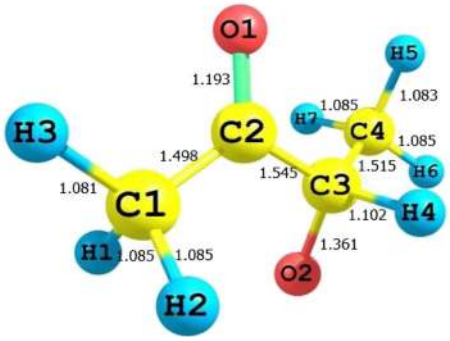

$CH_3COCH(O)CH_3$ (P3)

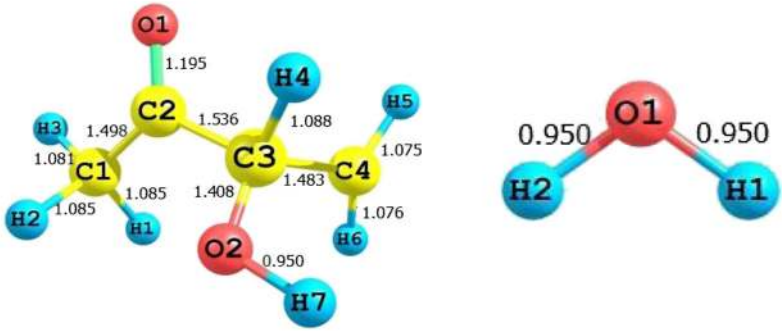

$CH_3COCH(OH)CH_2$ (P4)

Figure 1. (*continued*).

confirmation of the existence of transition states connecting reactants and products.

Single point energy calculations of various species involved in the hydrogen abstraction reactions were further refined by using CCSD(T)/6-311++G(d,p) level of theory at BHandHLYP/6-311++G(d,p) optimized geometries. Calculated total energies are corrected for zero-point energy obtained at BHandHLYP/6-

Table 2. Harmonic vibrational frequencies of reactant, reactant complexes, transition states, product complexes and products calculated at BHandHLYP/6-311++G (d,p) level of theory.

Species	Vibrational frequency (cm^{-1})
$CH_3COCH(OH)CH_3$	21, 158, 245, 258, 265, 318, 424, 499, 550, 626, 768, 940, 1009, 1022, 1093,1168, 1199, 1237, 1305, 1402, 1444, 1456, 1463, 1511, 1517, 1544, 1552, 1885, 3092, 3114, 3130, 3180, 3192, 3215, 3237, 4016
RC1a	29, 35, 62, 171, 188, 248, 258, 269, 311, 415, 459, 510, 552, 620, 664, 773, 940, 1008, 1032, 1089, 1163, 1185, 1257, 1318, 1403, 1446, 1455, 1461, 1513, 1525, 1546, 1552, 1888, 3112, 3125, 3126, 3179, 3189, 3216, 3236, 3725, 4002
RC1b	21, 35, 42, 158, 159, 242, 260, 273, 317, 425, 478, 506, 608, 631, 775, 941, 1010, 1027, 1095, 1168, 1203, 1243, 1313, 1399, 1448, 1458, 1467, 1511, 1515, 1544, 1552, 1862, 3094, 3117, 3130, 3183, 3192, 3216, 3239, 3711, 4016
RC2	29, 49, 61, 159, 172, 240, 258, 267, 315, 419, 455, 522, 549, 601, 630, 777, 943, 1007, 1032, 1092, 1167, 1202, 1241, 1318, 1401, 1449, 1460, 1467, 1508, 1517, 1547, 1549, 1865, 3103, 3115, 3132, 3181, 3193, 3214, 3241, 3720, 4015
RC3/RC4a	20, 30, 34, 100, 124, 160, 240, 247, 269, 327, 421, 450, 509, 553, 626, 772, 941, 1008, 1024, 1103, 1168, 1204, 1273, 1315, 1401, 1445, 1454, 1476, 1511, 1517, 1546, 1553, 1882, 3086, 3116, 3130, 3182, 3192, 3212, 3235, 3878, 3952
RC4b	28, 48, 60, 159, 171, 240, 258, 266, 314, 418, 454, 454, 522, 548, 601, 630, 777, 943, 1006, 1032, 1091, 1166, 1201, 1240, 1318, 1400, 1448, 1460, 1467, 1507, 1516, 1546, 1548, 1865, 3103, 3114, 3131, 3193, 3214, 3241, 3720, 4014
TS1a	1705i, 33, 38, 87, 170, 230, 233, 277, 343, 387, 434, 480, 552 ,637, 703, 782, 913, 943, 971, 1041, 1087, 1166, 1200, 1241, 1278, 1302, 1403, 1409, 1464, 1469, 1498, 1540, 1551, 1853, 3072, 3121, 3188, 3197, 3219, 3290, 3918, 4019
TS1b	2047i, 15, 39, 134, 232, 242, 257, 280, 327, 422, 424, 479, 553, 615, 683, 763, 877, 940, 999, 1056, 1101, 1151, 1197, 1205, 1239, 1305, 1400, 1451, 1459, 1472, 1538, 1544, 1550, 1865, 3095, 3116, 3175, 3183, 3215, 3247, 3884, 4014,
TS2	1086i, 20, 79, 117, 148, 235, 254, 289, 307, 330, 434, 489, 533, 618, 669, 757, 897, 962, 1021, 1028, 1102, 1159, 1228, 1247, 1298, 1405, 1450, 1457, 1497, 1510, 1517, 1537, 1548, 1869, 3113, 3130, 3178, 3192, 3224, 3239, 3898, 4002,
TS3	2519i, 36, 50, 127, 155, 221, 224, 241, 310, 411, 437, 508, 552, 637, 755, 814, 938, 1003, 1005, 1113, 1169, 1185, 1248, 1275, 1353, 1402, 1435, 1448, 1466, 1510, 1520, 1542, 1547, 1895, 3061,3127, 3130, 3190, 3201, 3223, 3236, 3946
TS4a	1654i, 15, 73, 117, 156, 222, 226, 311, 408, 427, 494, 537, 547, 625, 701, 752, 848, 943, 1019, 1054, 1154, 1192, 1219, 1266, 1310, 1328, 1407, 1418, 1447, 1486, 1502, 1512, 1517, 1880, 3085, 3131, 3171, 3194, 3237, 3261, 3930, 3937
TS4b	2027i, 24, 88, 153, 163, 254, 266, 316, 379, 428, 480, 494, 547, 633, 668, 767, 857, 991, 1015, 1059, 1102, 1147, 1192, 1240, 1246, 1293, 1399, 1445, 1472, 1503, 1509, 1515, 1518, 1874, 3085, 3131, 3159, 3193, 3240, 3242, 3858, 4012

Table 2. (continued)

Species	Vibrational frequency (cm^{-1})
PC1a	24, 27, 53, 95, 159, 221, 250, 261, 327, 411, 442, 445, 514, 552, 608, 656, 796, 848, 951, 1040, 1080, 1140, 1191, 1262, 1339, 1410, 1458, 1459, 1505, 1545, 1550, 1614, 1674, 3112, 3124, 3180, 3213, 3250, 3374, 3883, 3999, 4060
PC1b	40, 51, 82, 98, 156, 248, 254, 277, 334, 396, 421, 451, 526, 557, 584, 666, 803, 877, 952, 1056, 1079, 1145, 1202, 1250, 1345, 1407, 1458, 1467, 1520, 1544, 1550, 1623, 1680, 3099, 3114, 3181, 3213, 3245, 3375, 3840, 4016, 4056
PC2	29, 77, 92, 96, 109, 126, 172, 263, 335, 372, 373, 393, 514, 576, 587, 606, 748, 980, 1044, 1054, 1078, 1133, 1279, 1392, 1450, 1471, 1509, 1520, 1526, 1536, 1594, 1672, 1689, 3085, 3128, 3129, 3187, 3234, 3248, 3831, 3997, 4060
PC3	20, 51, 58, 108, 127, 145, 207, 262, 316, 332, 398, 446, 491, 542, 635, 740, 940, 946, 1001, 1085, 1143, 1153, 1200, 1253, 1319, 1449, 1468, 1510, 1521, 1540, 1545, 1667, 1898, 2964, 3128, 3135, 3190, 3209, 3229, 3237, 3919, 4064
PC4a	32, 38, 60, 89, 135, 142, 153, 218, 224, 240, 306, 418, 517, 558, 565, 632, 695, 803, 930, 1029, 1059, 1139, 1190, 1249, 1315, 1378, 1445, 1464, 1488, 1512, 1518, 1671, 1880, 3096, 3131, 3196, 3228, 3233, 3346, 3876, 3980, 4083
PC4b	42, 68, 95, 138, 142, 166, 237, 254, 293, 310, 389, 417, 532, 558, 567, 604, 638, 798, 943, 1026, 1057, 1140, 1181, 1231, 1322, 1366, 1433, 1448, 1508, 1517, 1680, 1861, 3122, 3132, 3196, 3226, 3237, 3354, 3841, 4006, 4058
$CH_2COCH(OH)CH_3$	51, 245, 259, 266, 334, 415, 445, 510, 549, 656, 792, 850, 951, 1045, 1077, 1146, 1200, 1245, 1331, 1409, 1458, 1464, 1505, 1544, 1550, 1617, 3099, 3113, 3179, 3212, 3250, 3377, 4017
$CH_3COC(OH)CH_3$	88, 127, 129, 255, 319, 340, 374, 503, 578, 591, 741, 975, 1038, 1053, 1077, 1131, 1273, 1392, 1448, 1460, 1504, 1520, 1526, 1535, 1583, 1670, 3084, 3125, 3127, 3184, 3231, 3235, 4001
$CH_3COCH\ (O)CH_3$	54, 146, 201, 253, 311, 401, 471, 531, 626, 726, 912, 947, 996, 1066, 1138, 1150, 1198, 1251, 1346, 1450, 1462, 1510, 1521, 1536, 1542, 1896, 2971, 3128, 3134, 3191, 3206, 3222, 3236
$CH_3COCH(OH)CH_2$	65, 142, 214, 231, 287, 307, 412, 521, 561, 568, 635, 796, 931, 1023, 1058, 1138, 1181, 1223, 1311, 1362, 1427, 1447, 1493, 1512, 1519, 1886, 3111, 3131, 3195, 3229, 3235, 3348, 4006
H_2O	1652, 3983, 4087
OH	3884

311G++(d,p) level. The associated energy barrier with zero-point energy correction for various species and transition states involved in the title reactions calculated at CCSD(T)/6-311++G(d,p) and BHandHLYP/6-311++G(d,p) methods are recorded in table 3. The results show that the calculation performed during the present study utilizing CCSD(T) yields the barrier height of 4.73, 4.80, -1.09, 4.49, 3.03 and 3.39 kcal mol^{-1}, respectively for reactions (R1–R4) whereas these values are 6.23, 6.61, 0.55, 6.28, 4.66 and 5.11 kcal mol^{-1}, respectively for TS1a, TS1b, TS2, TS3, TS4a and TS4b at BHandHLYP level. A schematic potential energy surface of the 3H2B + OH reactions are plotted and shown in figure 2. In the construction of energy diagram, relative energy including zero-point correction as recorded in table 3 are utilized. Literature survey reveals that there is no experimental data available for the comparison of the energy barrier for the H-atom abstraction reaction of 3H2B by OH radicals. However, our calculated barrier heights are

in reasonable agreement with the previous studies on hydrogen abstraction reactions of similar hydroxyacetone ($CH_3C(O)CH_2OH$) with OH radicals by Galano *et al.*,[15] Dillon *et al.*[16] and Baasandorj *et al.*[17] The reaction of hydroxyacetone with the OH radical is thought to proceed mainly by abstraction of a secondary H-atom from $–CH_2(OH)$ site.[15–17] Our calculation also confirms that the hydrogen abstraction from the –CH group attached to hydroxyl group is more facile than that from the other reaction channels. This finding is in line with the observation made in an earlier report,[23] as well as to the fact that the calculated C-H bond dissociation energy from –CH group (90.52 kcal mol^{-1}) is much lower than that for the other sites (cf. table 5). The thermodynamic parameters also reveal that H-abstraction from –CH group is kinetically more favourable than that of the other reaction channels. Moreover, spin contamination is not important for the 3H2B + OH reactions because $<S^2>$ is found to be 0.76 at BHandHLYP/6-311G++(d, p) before annihilation that is only slightly larger than the expected value of $<S^2> = 0.75$ for doublets.

The standard enthalpy of formation ($\Delta_fH^\circ_{298}$) at 298 K for 3H2B and the radicals generated from hydrogen abstraction, $CH_2COCH(OH)CH_3$ (P1), $CH_3COC(OH)CH_3$ (P2) $CH_3COCH(O)CH_3$ (P3) and $CH_3COCH(OH)CH_3$ (P4) can be valuable information for understanding the mechanism and thermochemical properties of their reactions and most importantly for atmospheric modeling, but these values are not yet reported. The group-balanced isodesmic reactions, in which the number and types of bonds are conserved, are used as working chemical reactions herein to calculate the $\Delta_fH^\circ_{298.}$ Here, four isodesmic reactions are used to estimate the enthalpies of formation of the $CH_3COCH(OH)CH_3$. The used isodesmic reactions are as follows:

$$CH_3COCH(OH)CH_3 + CH_4 \rightarrow CH_3COCH_3 + CH_3CH_2OH \quad (R5)$$
$$CH_3COCH(OH)CH_3 + CHF_3 \rightarrow CH_3C(O)OH + CF_3CH_2CH_3 \quad (R6)$$
$$CH_3COCH(OH)CH_3 + CH_3 \rightarrow CH_2C(O)CH_2CH_3 + CH_3OH \quad (R7)$$
$$CH_3COCH(OH)CH_3 + CH_3CH_3 \rightarrow CH_3C(O)CH_2CH_3 + CH_3CH_2OH \quad (R8)$$

Table 3. Zero-point energy corrected associated energy barriers, ΔE in kcal mol^{-1} of reactant, reactant complexes, transition states, product complexes and products at CCSD (T)/6-311++G(d,p) and BHandHLYP/6-311++G(d,p) levels of theory.

Species	CCSD(T)	BHandHLYP
$CH_3COCH(OH)CH_3$+ OH	0.00	0.00
RC1a	−3.12	−4.12
RC1b	−3.32	−5.54
RC2	−3.50	−5.50
RC3/RC4a	−2.10	−3.16
RC4b	−3.80	−4.70
TS1a	4.73	6.23
TS1b	4.80	6.60
TS2	−1.09	0.55
TS3	4.49	6.28
TS4a	3.03	4.66
TS4b	3.39	5.11
PC1a	−22.20	−21.98
PC1b	−23.30	−23.89
PC2	−36.48	−38.77
PC3	−14.20	−15.18
PC4a	−18.79	−17.29
PC4b	−19.01	−17.47
$CH_2COCH(OH)CH_3$(**P1**) + H_2O	−18.46	−18.93
$CH_3COC(OH)CH_3$(**P2**) + H_2O	−30.83	−33.08
$CH_3COCH(O)CH_3$(**P3**) + H_2O	−10.94	−12.32
$CH_3COCH(OH)CH_2$(**P4**) + H_2O	−13.33	−12.07

All geometrical parameters of the species involved in the isodesmic reactions (R5–R8) were first optimized at the BHandHLYP/6-311++G(d,p) level and then energies of the species were further refined by performing single-point calculations at the sophisticated CCSD(T) level of theory. At first, we have calculated the reaction enthalpies ($\Delta_rH^\circ_{298}$) of the isodesmic reactions (R5–R8) as mentioned above, using total energies of the species obtained at CCSD(T)/6-311++G(d,p) level and including thermal correction to enthalpy estimated at BHandHLYP/6-311++G(d,p) level. Since, the ($\Delta_rH^\circ_{298}$) value corresponds to the difference of the enthalpy of formation ($\Delta_fH^\circ_{298}$) values between the products and the reactants, the ($\Delta_fH^\circ_{298}$) values of the reactant and product species are easily evaluated by combining them with the known enthalpies of formation of the reference compounds involved in our isodesmic reaction schemes. The experimental $\Delta_fH^\circ_{298}$ values for CH_4: −17.89 kcal mol^{-1}, CH_3COCH_3: −51.9 kcal mol^{-1}, CH_3CH_2OH: −56.23 kcal mol^{-1}, CH_3CH_3: − 20.24 kcal mol^{-1}, CH_3:34.82 kcal mol^{-1} $CH_2C(O)CH_2CH_3$: −13.57 kcal mol^{-1}, $CH_3C(O)CH_2CH_3$: −57.02 kcal mol^{-1}, CH_3OH: −48.08 kcal mol^{-1} are taken from Ref. [2], CHF_3: − 166.60 kcal mol[39], $CH_3C(O)OH$: −103.44 kcal mol[40], $CF_3CH_2CH_3$: −183.09 kcal mol[41] to evaluate the required enthalpies

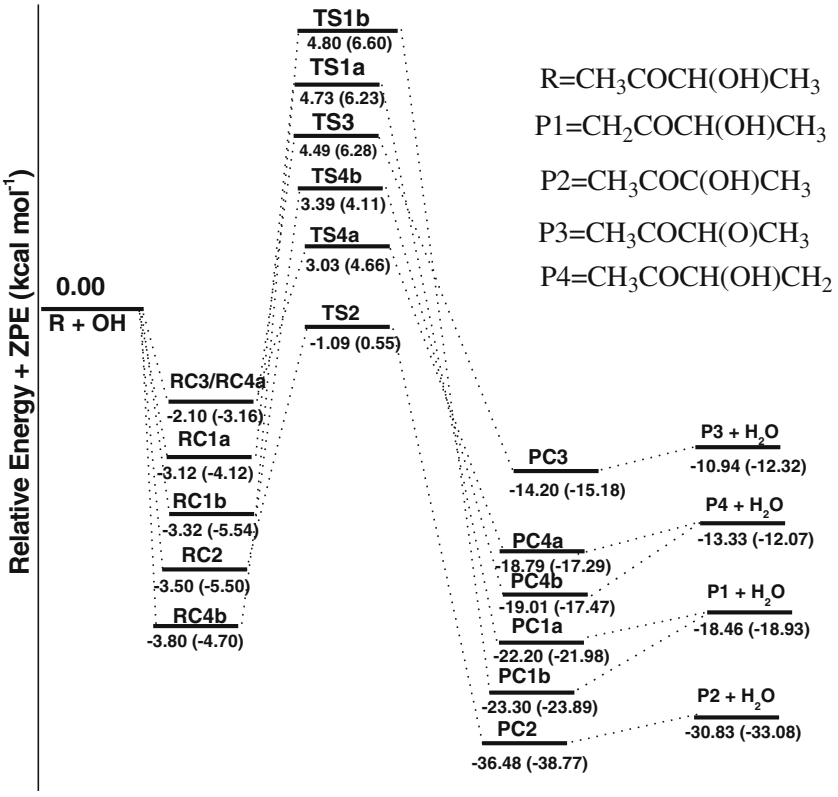

Figure 2. Schematic potential energy profiles (including ZPE) for the 3H2B + OH reactions at the CCSD(T)/6-311++G(d,p) level. The values given in parentheses are calculated at BHandHLYP/6-311++G(d,p) + ZPE level of theory.

of formation. The calculated values of enthalpies of formation are listed in table 4. The $\Delta_f H^\circ_{298}$ for 3H2B calculated from CCSD(T) and BHandHLYP results are −96.23 and −93.23 kcal mol^{-1}, respectively. The $\Delta_f H^\circ_{298}$ values for radicals generated by hydrogen abstraction (P1, P2, P3 and P4) can also be easily calculated from the reported $\Delta_r H^\circ_{298}$ values for reactions R1–R4 in table 1, the calculated $\Delta_f H^\circ_{298}$ value for 3H2B and the experimental $\Delta_f H^\circ_{298}$ values for H_2O (−57.8 kcal mol^{-1}) and OH (8.93 kcal mol^{-1}) radical[2]. The $\Delta_f H^\circ_{298}$ values for P1, P2, P3 and P4 radicals calculated from the CCSD(T) results are −45.79, −57.85, −38.19 and −40.29 kcal mol^{-1}, respectively; whereas for the same BHandHLYP results amount to −45.46, −59.30, −38.77 and −38.23 kcal mol^{-1}, respectively. Moreover, because of the lack of experimental values for the $\Delta_f H^\circ_{298}$ of the species involved in the title reactions, it is difficult to make a direct comparison between theoretical and experimental enthalpy of formation. Since, these data are not available in the literature and can therefore be useful for further thermochemical and kinetic modeling of reaction involving these species.

Table 4. Enthalpies of formation ($\Delta_f H^0_{298}$) (kcal mol^{-1}) for species at CCSD(T) and BHandHLYP/6-311++G(d,p) levels of theory.

Species	Isodesmic Reaction Schemes	CCSDT	BHandHLYP
3H2B	R5	−96.03	−93.29
	R6	−94.96	−91.91
	R7	−98.06	−93.70
	R8	−96.05	−94.14
Average		−96.27	−93.26
$CH_2COCH(OH)CH_3$(**P1**)		−45.79	−45.46
$CH_3COC(OH)CH_3$(**P2**)		−57.85	−59.30
$CH_3COCH(O)CH_3$(**P3**)		−38.19	−38.77
$CH_3COCH(OH)CH_2$(**P4**)		−40.29	−38.23

The calculated bond-dissociation energies, BDE (D^0_{298}) of the C-H bonds of $CH_3COCH(OH)CH_3$ molecule are recorded in table 5. The D^0_{298} value obtained from the CCSD(T) results for the C–H bonds in the $–CH_3C(O)$, −CH(attached to hydroxyl group), −OH and $–CH_3$ sites of 3H2B amount to 102.58, 90.52, 110.18 and 108.08 kcal mol^{-1}, respectively. The D^0_{298} values obtained from BHandHLYP/6-311++G(d,p) results amount to be 99.90, 86.07, 106.59 and 107.13 kcal mol^{-1}, respectively. No comparison between theory and experiment can be made due to the lack of the

Table 5. Calculated bond dissociation energy (D^0_{298}) (kcal mol^{-1}) for species at 298 K at CCSD(T) /6-311++G(d,p) and BHandHLYP/6-311++G(d,p) levels of theory.

Bond dissociation type	CCSD(T)	BHandHLYP
C-H bond		
$CH_3COCH(OH)CH_3 \rightarrow CH_2COCH(OH)CH_3 + H$	102.58	99.90
$CH_3COCH(OH)CH_3 \rightarrow CH_3COC(OH)CH_3 + H$	90.52	86.07
$CH_3COCH(OH)CH_3 \rightarrow CH_3COCH(O)CH_3 + H$	110.18	106.59
$CH_3COCH(OH)CH_3 \rightarrow CH_3COCH(OH)CH_2 + H$	108.08	107.13

experimental D^0_{298} values. However, our calculated D^0_{298} value for the four C-H bonds of 3-hydroxy-2-butanone is in reasonable agreement with calculated D^0_{298} values for the C-H bonds in a similar ketone (3-methyl-2-butanone) reported by Hudzik and Bozzelli.[42] Moreover, owing to the lower C-H bond dissociation energy; CH site attached to hydroxyl group is more reactive toward hydrogen abstraction than other sites. This is reflected in the calculated barrier height for hydrogen abstraction from $–CH_3C(O)$, CH (attached to hydroxyl group) -OH and $–CH_3$ groups.

3.1 *Rate constants*

The rate constant for reactions channels (R1–R4) are calculated by using Canonical Transition State Theory[43] given by the following expression:

$$k = \sigma\Gamma(T)\frac{k_B T}{h}\frac{Q_{TS}}{Q_A . Q_B}\exp\frac{-\Delta E^{\#}}{RT} \qquad (1)$$

Where, σ is the number of equivalent H-atoms, $\Gamma(T)$ is the tunneling correction factor at temperature T. Q_{TS}, Q_A and Q_B are the total partition functions (per unit volume) for the transition states and reactants, respectively. $\Delta E^{\#}$ is the barrier height including zero point energy correction, k_B is the Boltzmann constant, h is the Planck's constant and R represents the universal gas constant. The tunneling correction was estimated by using the Eckart's unsymmetrical barrier method.[44] All vibrational modes, except the lowest vibrational mode, were treated quantum mechanically as separable harmonic oscillators, whereas for the lowest-frequency mode, the partition function was evaluated by the hindered-rotor approximation by Truhlar and Chuang[45] method. Using Truhlar's procedure[46] the q^{HIN}/q^{HO} ratio was found to be close to unity. Some of the low lying vibrational frequencies that are included in the Qvib are termed as internal rotations. In this type of rotation, one part of the molecule rotates with respect to the other part in torsion angle. Such a rotor may be treated in three different ways depending on the rotational barrier. If barrier to rotation is much lesser than the room temperature energy, kT or 207 cm^{-1}, then the rotation is treated as a free rotor. On the other hand, if the barrier is much larger than kT, then the rotation would be treated as harmonic oscillator or as a normal harmonic vibration. In the intermediate cases where the torsional barrier is comparable to kT, the rotation is treated as hindered-rotor. The harmonic contribution of these internal rotations to the vibrational partition function is written as Q_{IR}. In order to consider the harmonic contribution of these internal rotations to the vibrational partition function, the harmonic contribution of the vibrations due to hindered and free rotors were eliminated from the vibrational partition function Q_{vib} of reactants and transition states and the corrected vibrational partition function for reactants and transition states were evaluated using the following expression:

$$Q_{corr} = \frac{Q_{HO} \cdot Q_{IR}}{\Pi_{Qv=i}}$$

Where, Q_{HO} is the harmonic oscillator partition function, Q_{IR} the internal rotation partition function and $Q_{v=i}$ is the partition function of normal mode vibrations corresponding to internal rotation. During the calculation of total partition function for OH radical, its electronic partition function was corrected by considering the excited state of OH radical with a 140 cm^{-1} splitting by using the expression given below:

$$Q^E(OH) = 2 + 2\exp\left[-\frac{140\left(cm^{-1}\right)hc_0}{k_b T}\right] \qquad (2)$$

The partition functions for the respective transition states and reactants at any temperature are calculated with rigid rotor and harmonic oscillator approximations and the vibrational frequencies obtained from the BHandHLYP/6-311++G(d,p) level are used. As discussed before, the H-abstraction by OH radicals proceeds via a two-step mechanism. The first step involves a fast pre-equilibrium (K_{eq}) between the reactants and the hydrogen bonded reaction complex (RC) and the second step is the hydrogen abstraction with the rate constant $k_2^{\dagger}$. The overall rate constant including

equilibrium constant (K_{eq}) and rate constant $\left(k_2^{\dagger}\right)$ are given by,

$$K_{eq} = \frac{Q_{RC}}{Q_A \cdot Q_B} e(E_R - E_{RC})/RT \quad (3)$$

and $k_2^{\dagger}$ can be obtained from Eq. 4

$$k_2^{\dagger} = \sigma \Gamma (T) \frac{k_B T}{h} \frac{Q_{TS}}{Q_{RC}} e^{-(E_{TS}-E_{RC})/RT} \quad (4)$$

The rate constant for H-abstraction from 3H2B via reaction (R1) is then obtained by the following expression,

$$k = K_{eq} \times k_2^{\dagger} = \sigma \Gamma (T) \frac{k_B T}{h} \frac{Q_{TS}}{Q_A \cdot Q_B} e - \frac{E_{TS} - E_R}{RT} \quad (5)$$

where Q_A, Q_B, Q_{RC} and Q_{TS} represents the total partition functions (per unit volume) of the reactants, reaction complex and transition states, respectively. E_{TS}, E_{RC} and $E_R$are the total energies (ZPE corrected) of transition state, reaction complex and reactants, respectively. Thus, it seems that the final expression (Eq. 5) for estimating rate constant and barrier height turns out to be the usual CTST expression (Eq. 1) used for the determination of rate constant and barrier height of a direct reaction, irrespective of the energy of pre-reactive hydrogen bonded complex (RC). Of course, the formation of pre and post-reaction complexes modify the shape of potential energy surface for the reaction and hence affects the tunneling factor. As a result, the rate constant for hydrogen abstraction reactions also changes. In our case, the rate constant is seen to increase by 1.3 to1.6 times at 298 K compared to the rate constant value for direct reaction from reactants to products due to greater tunneling factor. The branching ratios for the H-abstraction reaction channels, which represent their individual contribution towards overall reaction rate has been determined by using the following expression,

$$\text{Branching ratio} = \frac{k}{k_{total}} \times 100 \quad (6)$$

The partial rate coefficients cannot be determined experimentally because reactions occur simultaneously, and in some cases they even lead to the same products. Thus, the experimental data are mostly available only for the overall reactions. That is why theoretical methods can be so valuable for the full understanding of the chemical systems. As stated earlier, 3H2B + OH reactions pass through four different channels (R1–R4) the contribution from each of these channels needs to be taken into account while calculating the total rate coefficient (k_{OH}) for the titled reaction. The total rate coefficient (k_{OH}) is therefore, obtained from the addition of rate coefficients for the four channels: k_{OH} = (kR1a + kR1b) + kR2 + kR3 + (kR4a + kR4b). The calculated total rate constant (k_{OH}) values for hydrogen abstraction reactions of 3H2B with OH radicals within a range of temperature 250–450 K along with experimental data are presented in table 6. It can be seen from table 6 that our calculated k_{OH} value at 298 K using CCSD(T)/6-311++G(d,p) barrier heights is 1.20 × 10^{-11} cm^3 $molecule^{-1}$ s^{-1} which is in good agreement with the experimental value of 1.03 × 10^{-11} and 0.96 × 10^{-11} cm^3 $molecule^{-1}$ s^{-1} reported by Aschmann *et al.*[14] and Messaadia *et al.*[23], respectively. The calculated rate constant values for the reaction between 3H2B with OH radicals in the temperature range of 250–450 K is fitted in the two parameter model eqn. and found to be well described by the following equation:

Table 6. The total rate constant values k_{OH} (in cm^3 $molecule^{-1}s^{-1}$) for hydrogen abstraction reactions of 3H2B with OH radicals using CCSD(T)/6-311++G(d,p) barrier heights.

T(K)	k_{OH}	Exp. values
250	0.856E-11	
298	1.20E-11	1.03E-11[a]; 0.96E-11[b]
300	1.22E-11	
350	1.54E-11	
400	1.91E-11	
450	2.25E-11	

[a]Aschmann *et al.*[14]; [b]Messaadia *et al.*[23]

$$k_{OH} = 7.56 \times 10^{-11} \exp[-(549.3 \pm 11.2)/T] \quad (7)$$

The correlation coefficient (R^2) value for the fitting is 0.998 indicating the goodness of this model equation in representing the rate constant values in the said temperature range. The branching ratios for reactions (R1–R4) are calculated using Eq. (6) and found to be 2.0%, 93.0%, 1.8% and 3.2%, respectively at 298 K. The calculated branching ratio values clearly indicate the dominance of H-abstraction from –CH group attached to hydroxyl group to the overall rate constant compare to its counterparts. Hence our calculation predicts reaction R2 as the major reaction channel as observed from the experimental study of Messaadia *et al.*[23]

3.2 *Atmospheric implications*

The atmospheric lifetime of 3H2B (τ_{eff}) can be estimated by assuming that its removal from the atmosphere occurs primarily through the reaction with OH radicals. Then τ_{eff} can be expressed as:[47]

$$\tau_{eff} \approx \tau_{OH}$$

Where, $\tau_{OH} = \left(k_{OH} \times [OH]^{-1}\right)$ and [OH] is the global average OH radical concentration in atmosphere. Taking the global average atmospheric OH radical concentration of 1.0×10^6 molecules cm[48] and k_{OH} value at 298 K as 1.20×10^{-11}cm^3 molecule^{-1}s^{-1}, the atmospheric lifetime of 3H2B is estimated to be 1.04 days which is in very good agreement with the experimentally reported atmospheric lifetime of 3H2B with respect to the reaction with OH radicals by Messaadia *et al*.[23] (1.2 days).

4. Conclusions

We present here the potential energy profiles (including geometries, energies and vibrational frequencies of reactant, transition states and products) and kinetic data of H atom abstraction reaction of 3H2B with OH radical investigated at the CCSD(T)//BHandHLYP/6-311++G(d,p) level of theory. All the reactions were found to proceed by an indirect mechanism through formation of hydrogen bonded pre- and post-reaction complexes. The barrier height for reaction channels (R1–R4) calculated at CCSD(T)/6-311++G(d,p) level were found to be 4.73, 480, −1.09, 4.49, 3.03 and 3.39 kcal mol^{-1}, respectively. The overall rate constant for the H atom abstraction of 3H2B by OH radicals was found to be 1.20×10^{-11} cm^3 molecule^{-1} s^{-1} at 298 K which is in good agreement with the available experimental data. A model equation has been proposed to describe the rate coefficients in a wide temperature range of 250–450 K as $k_{OH} = 7.56 \times 10^{-11}\exp[-(549.3 \pm 11.2)/T]$ cm^{-3} molecule^{-1} s^{-1}. The branching ratio results show that hydrogen abstraction from –CH group attached to hydroxyl group (R2) is thermodynamically and kinetically more facile than that of other reaction channels. This is further ascertained by bond dissociation energy calculation for –C-H bonds. The $\Delta_f H^0_{298}$ values for 3H2B and $CH_2COCH(OH)CH_3$, $CH_3COC(OH)CH_3$, $CH_3COCH(O)CH_3$, and $CH_3COCH(OH)CH_3$ radicals were calculated for the first time and found to be −96.23, 45.79, −57.85, −38.19 and −40.29 kcal mol^{-1}, respectively at CCSD(T)/6-311++G(d,p) level. Atmospheric lifetime of 3H2B was estimated to be 1.04 days. These data can be useful for further thermo-kinetic modeling of other reactions involving these species.

Acknowledgements

BKM is thankful to University Grants Commission, New Delhi for providing Dr. D. S. Kothari Fellowship. NKG and HJS are thankful to Council of Scientific and Industrial Research (CSIR), New Delhi for providing financial assistance.

References

1. Mendes J, Zhou C W and Curran H J 2013 *J. Phys. Chem. A* **117** 4515
2. Sebbar N, Bozzelli J W and Bockhorn H 2014 *J. Phys. Chem. A* **118(1)** 21
3. Wolfe G M, Crounse J D Parrish J D, Clair J M St, Beaver M R, Paulot F, Yoon T P, Wennberg P O and Keutsch F N 2012 *Phys. Chem. Chem. Phys*. **14** 7276
4. El Dib G, Sleiman C, Canosa A, Travers D, Courbe J, Sawaya T, Mokbel I, and Chakir A 2013 *J. Phys. Chem. A* **117** 117
5. Wildt J, Kobel K, Schuh-Thomas G and Heiden A C 2003 *J. Atmos. Chem.* **45** 173
6. Schauer J J, Kleeman M J, Cass G R, and Simoneit B R T 2001 *Environ. Sci. Technol*. **35** 1716
7. Baugh J, Ray W, Black F and Snow R 1987 *Atmos. Environ*. **21** 2077
8. de Andrade M V A S, Pinheiro H L C, Pereira P A D and de Andrade J B 2002 *Quim. Nova*. **25** 1117
9. Calvert J G and Madronich S J 1987 *Geophys. Res.* **92** 2211
10. Mousavi M and Seyfi H 2011 *Org. Chem. J.* **1** 17
11. Koprowski M, Luczak J and Krawczyk E 2006 *Tetrahedron* **62** 12363
12. Hayakawa R, Sahara T and Shimizu M 2000 *Tetrahedron Lett*. **41** 7939
13. Palomo C, Oiarbidea M and Garcıa J M 2012 *Chem. Soc. Rev.* **41** 4150
14. Aschmann S M, Arey J and Atkinson R 2000 *J. Phys. Chem. A* **104** 3998
15. Galano A 2006 *J. Phys. Chem. A* **110** 9153
16. Dillon T J, Horowitz A, Holscher D, Crowley J N, Vereecken L and Peeters J 2006 *Phys. Chem. Chem. Phys.* **8** 236
17. Baasandorj M, Griffith S, Dusanter S and Stevens P S 2009 *J. Phys. Chem. A* **113** 10495
18. Messaadia L, El Dib G, Ferhati A, Roth E and Chakir A 2012 *Chem. Phys. Lett*. **529** 16
19. Butkovskaya N I, Pouvesle N, Kukui A, Liu R Z and Bras G L 2006 *J. Phys. Chem. A* **110** 13492
20. Baker J, Arey J and Atkinson R 2004 *J. Phys. Chem. A* **108** 7032
21. Wu Y Y, Chen K, Pan D T, Zhu J W, Wu B and Shen Y L 2011 *J. Chem. Eng. Data* **56** 2641
22. Wren J C and Glowa G A 2000 *Radiat. Phys. Chem*. **58** 341
23. Messaadia L, El Dib G, Lender M, Cazaunau M, Roth E, Ferhati A, Mellouki A and Chakir A 2013 *Atmos. Environ*. **77** 951
24. Becke A D 1993 *J. Chem. Phys*. **98** 1372
25. Lee C, Yang W and Parr R G 1988 *Phys. Rev. B* **37** 785
26. Yu A Y and Zhang H X 2013 *J. Mol. Model*. **19** 4503
27. Prasanthkumar K P, Suresh C H and Aravindakumar C T 2013 *J. Phys. Org. Chem*. **26** 510
28. Prasanthkumar K P, Suresh C H and Aravindakumar C T 2012 *J Phys Chem A* **116** 10712

29. Galano A. Alvarez-Idaboy J R and Francisco-Marquez M 2010 *J. Phys. Chem. A* **114** 7525
30. Gonzales C and Schlegel H B 1991 *J. Chem. Phys.* **95** 5853
31. Scuseria G E and Schaefer H F 1989 *J. Chem. Phys*. **90** 3700
32. Pople J A, Gordon M H and Raghavachari K 1989 *J. Chem. Phys*. **87** 5968
33. Mishra B K, Chakrabartty A K, Bhattacharjee D and Deka R C 2013 *Struct. Chem*. **24** 1621
34. Mishra B K, Chakrabartty A K and Deka R C 2013 *Mol. Phys.* **112** 1512. doi: 10.1080/00268976.2013.842008
35. Gomez M C, Iuga C and Alvarez-Idaboy J R 2012 *Int. J. Quant. Chem*. **112** 3508
36. Ang-yang Yu 2014 *Struct. Chem.* **25** 607
37. Frisch M J *et al*. Gaussian 09 Revision- B.01 Gaussian, Inc., Wallingford C T, 2009
38. Hammond G S 1955 *J. Am. Chem. Soc*. **77** 334
39. Chase M W Jr. 1998 *J. Phys. Chem. Ref. Data Monograph* **9** 1
40. DeTar D F 1991 *J. Org. Chem*. **56** 1478
41. Yamada T, Bozzelli J W and Berry R J 1999 *J. Phys. Chem. A* **103** 5602
42. Hudzik J M and Bozzelli J W 2012 *J. Phys. Chem. A* **116** 5707
43. Laidler K J 2004 In *Chemical kinetics*, 3rd edn. (Delhi: Pearson Education)
44. Johnston H S and Heicklen J 1962 *J. Phys. Chem.* **66** 532
45. Chuang Y Y and Truhlar D G 2000 *J. Chem. Phys.* **112** 1221
46. Truhlar D G 1991 *J. Comput. Chem*. **12** 266
47. Papadimitriou V C, Kambanis K G, Lazarou Y G and Papagiannakopoulos P 2004 *J. Phys. Chem. A* **108** 2666
48. Atkinson R 1997 *J. Phys. Chem. Ref. Data* **26** 215